KSME

Springer

Journal of Mechanical Science and Technology 35 (4) 2021

Original Article
DOI 10.1007/s12206-021-0310-0

Keywords:
· Pipeline steel
· Fatigue life
· Fracture toughness
· Fatigue crack growth
· Hydrogen embrittlement
· Surface crack

Correspondence to:
Un Bong Baek
ubbaek@kriss.re.kr

Citation:
Nguyen, T. T., Heo, H. M., Park, J., Nahm, S. H., Beak, U. B. (2021). Fracture properties and fatigue life assessment of API X70 pipeline steel under the effect of an environment containing hydrogen. Journal of Mechanical Science and Technology 35 (4) (2021) 1445~1455.
http://doi.org/10.1007/s12206-021-0310-0

Received September 29th, 2020
Revised December 14th, 2020
Accepted December 17th, 2020

† Recommended by Editor Chongdu Cho

Fracture properties and fatigue life assessment of API X70 pipeline steel under the effect of an environment containing hydrogen

Thanh Tuan Nguyen, Hyeong Min Heo, Jaeyeong Park, Seung Hoon Nahm and Un Bong Beak

Research Team of Material Compatibility to Hydrogen Facility, Safety Measurement Institute, Korea Research Institute of Standard and Science, 267 Gajeong-Ro, Yeseong-Gu, Daejeon 34113, Korea

Abstract A series of fracture toughness and fatigue crack growth rate tests were performed on the X70 pipeline steel base and weld metals under 10 MPa of a natural/hydrogen gas mixture with 1 % H_2 blends. It is observed that the 10 MPa gas mixture with 1 % H_2 causes a significant reduction in the fracture toughness in both metals. The fatigue crack growth rates are markedly accelerated under the gas mixtures with 1 % hydrogen blend compared with the tests performed in ambient air. The obtained fracture parameters serve as inputs for fatigue life assessment analyses under the effect of a hydrogen-containing environment. The observed design fatigue life depends strongly only on the environmental conditions. The design fatigue strength of the structural pipeline exposed to hydrogen is much shorter than that under ambient air owing to the decrease in fracture toughness properties and acceleration of the fatigue crack growth rate.

1. Introduction

Natural gas (NG) has been widely used in the last several decades as an environmentally friendly energy source. Even though the development of new commercial renewable energy sources such as solar, wind, and hydrogen are expected to accelerate over the next decades, the use of NG is still expected to constitute an increasingly important part of world energy consumption because its reserves can meet the forecasted demand [1, 2]. However, the use of NG often faces the logistical challenge that it must be transported over long distances from the original extraction point to reach the final consumer. Therefore, pipeline infrastructure and maintenance are often associated with considerable cost. On the other hand, NG is an extremely flammable substance and its structural transportation pipelines often operate under conditions of high pressure and severe cyclic loading. Failure of these structural pipelines may cause economic losses and risks to human life. Safety issues such as leakage and explosion are always present during natural gas production and transportation [3-5]. It has been reported that the major problems occurring in the transport of natural gas through pipeline systems are often related to environmental cracking, such as stress corrosion or hydrogen-induced cracking [6-8]. Proper safety precautions and regulations for the practical use of structural pipeline systems have become a challenging issue for commercialized systems utilizing NG.

In general, high-strength low-alloy steels are most commonly used for constructing natural gas and sewage systems. The excellent strength and toughness of this group of materials allow them to withstand higher pressures and decrease the pipe thickness. They also have good weldability, which can provide lower installation and repair costs. However, it has been extensively reported that this type of structural pipeline steel is sensitive to various forms of environmental attachment, which may degrade the mechanical properties of the transportation materials [6-11]. The higher strength of the materials may increase their susceptibility to hydro-

gen embrittlement (HE). The actual condition of the NG may include a small portion of unfavorable components such as hydrogen sulfide or hydrogen, which can also be introduced into the materials through exposure to an aqueous hydrogen sulfide (H_2S)-containing environment [12-14]. Moreover, the use of hydrogen energy as a carrier energy has been introduced in many countries, necessitating its transportation through existing pipeline structures. Therefore, the safety regarding hydrogen-assisted fracture of pipelines has become a challenging issue for commercialized NG-utilizing systems. There is a strong need to improve the understanding of the mechanical behavior of pipeline steels in hydrogen-containing environments in order to derive safety guidelines for the design of these pipelines [15, 16].

In general, nondestructive inspection is the primary step necessary for the residual life assessment of pipelines, and this step is used to detect any potential defects, such as the length of defect flaw initiations existing in the structural components. Continuing to use a structural component with a defect crack may present a large hazard risk and is cause for concern [17-19]. The situation can become more serious under a synergistic effect between the severe stress conditions and hash environmental factors [20, 21]. It has been reported that the presence of any defect flaw may induce more HE susceptibility, as a high stress/strain concentration at the defect can enhance the hydrogen diffusion rate, causing the critical hydrogen concentration for hydrogen environmental assisted cracking to be achieved more readily [22, 23]. Assessment of the remaining life of a component containing a defect is necessary to ensure that the material is eligible for service under current standards. Moreover, high-pressure pipeline structures are often subjected to severe cyclic loading conditions. The understanding of fatigue crack growth behavior is important for the life prediction of structural components and should be carefully considered for safe design. Although modern numerical techniques using the finite element analysis method have been developed to predict the fatigue crack propagation process [24-26], the implementation procedures for fatigue life assessment using analytical solutions are still convenient for use in fundamental evaluation methods.

In this study, the effects of a natural gas environment containing hydrogen on the fracture toughness, K_{IC} and fatigue crack growth rate (FCGR) properties of X70 pipeline steel are investigated. The hydrogen-induced deterioration of the fracture parameters is characterized by changes in the fracture mechanism. Under this fracture mechanics-based approach, the fatigue life assessment of a high-pressure structural pipeline is demonstrated under various environmental conditions.

2. Effect of hydrogen on fracture properties

2.1 Material and experimental procedures

The material used in this research was API 5L X 70 pipeline steel, which is the structural pipeline material most commonly used for the transmission of natural gas in pipeline systems. The chemical composition is listed in Table 1. The specimens for fracture toughness and FCGR testing were extracted from a real pipeline component with an external diameter of 762 mm and a thickness of 12.7 mm in the transverse-longitudinal direction, as shown in Fig. 1(a). The fracture toughness test was carried out by measuring the crack-tip opening displacement (CTOD) using 0.5 compact tension (CT) specimens in accordance with ISO 111140 [27]. The load line displacement rate was 1 mm/min. FCGR tests were carried out on 1.0 CT specimens with the thickness of specimen was reduced by half (12.7 mm) in accordance with ASTM standard E647, with a frequency of 1 Hz and a load ratio of R = 0.1 in the load control [28]. Before the tests, a fatigue pre-crack was introduced into the specimen at the notch tip through cyclic loading. During the test, a clip gauge was applied to measure the crack opening displacement. After completing the tests, the specimens were fractured at liquid nitrogen temperatures to evaluate the average length of crack propagation. Details regarding the geometry of the tested specimens and the experimental procedure have been presented in previous research [29, 30].

The tests were performed at room temperature (25 °C) in ambient air and under a 10 MPa CH_4/H_2 gas mixture containing

Table 1. Chemical compositions of the API X70 pipeline steel, wt.%.

C	Mn	P	S	Cr	Ni	Cu
0.07	1.68	0.012	0.01	0.07	0.14	0.10

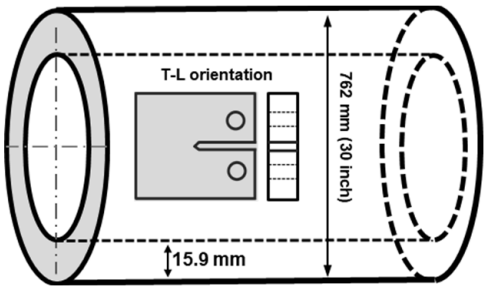

(a)

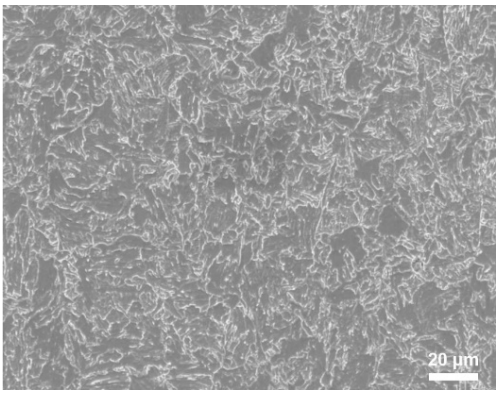

(b)

Fig. 1. (a) Pipe dimensions and specimen layout; (b) typical microstructure of the API X70 pipeline steel observed by SEM.

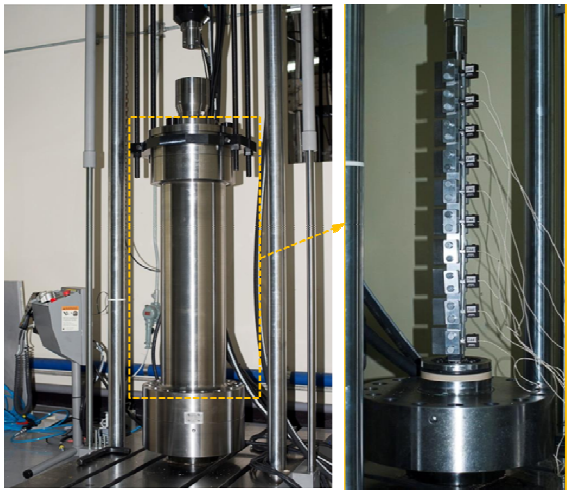

Fig. 2. Mechanical system used for fracture toughness and FCG testing under high-pressure hydrogen.

1 % H_2. The use of this hydrogen concentration was motivated by the small hydrogen concentrations that can be introduced into materials through electrochemical reactions in the pipeline cathodic protection process or in the form of H_2S. To simplify the experimental procedure, the gas mixture was preordered from an outside vendor before charging. The testing equipment was a specially designed autoclave with a maximum pressure of 120 MPa installed on a servo-hydraulic material testing frame, as depicted in Fig. 2. The system was also able to handle multiple specimens simultaneously. The load was measured by a load cell located inside the autoclave, and the crack open mouth displacement were measured using clip-on extensometers inside the pressure vessel. Prior to starting the test, an initial procedure including the creation of vacuum conditions and purging with high-purity helium and the corresponding gas was repeated at least three times to ensure gas purity. The fracture surface and fracture characteristics were analyzed via scanning electron microscopy (SEM) after the tests.

2.2 Effect of hydrogen on fracture toughness

A comparison of the CTOD and the corresponding fracture toughness values under ambient conditions and in 1 % H_2 is presented in Fig. 3 and Table 2. The equation for the relationship between the CTOD and K_{IC} values is expressed as follows:

$$\delta = \frac{4}{\pi} \frac{K_{IC}^2}{\sigma_y E} \quad (1)$$

where σ_y is the yield strength, and E is the Young's modulus, which was reported in previous studies [29]. On this basis, the variability in the fracture toughness, K_{IC}, has a similar tendency as the CTOD results. The CTOD of the specimen under ambient air is approximately 0.42 mm, which corresponds to an equivalent K_{IC} of 204 MPa·m$^{1/2}$. However, these values are

Table 2. CTOD and fracture toughness under three environmental conditions.

Test condition	CTOD (mm)	K_{IC} (MPa·m$^{1/2}$)
atm, RT	0.423	204.8
10 MPa, 1 % H_2	0.210	144.2
10 MPa, 100 % H_2	0.110	104.2

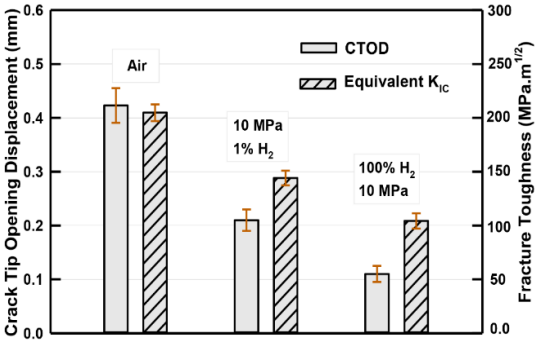

Fig. 3. Change in the fracture toughness and fatigue crack growth properties under three hydrogen-containing environments.

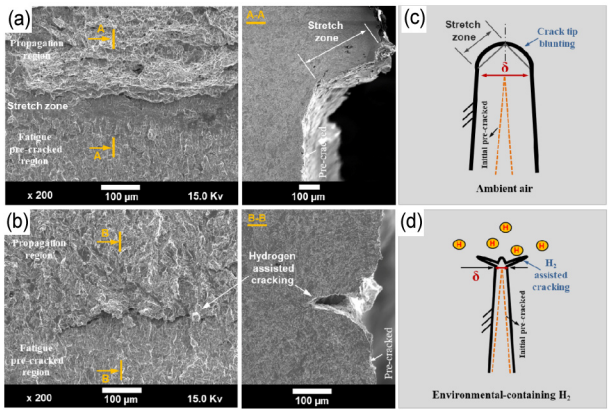

Fig. 4. Change in the fracture toughness and fatigue crack growth properties under two hydrogen-containing environments: (a) and (c) under ambient air; (b) and (d) under 1 % H_2 gas mixture at 10 MPa.

decreased markedly to approximately 0.21 mm and 144.2 MPa·m$^{1/2}$, respectively, when the specimen is tested in 1 % H_2 gas mixture conditions.

The influence of hydrogen on the crack initiation behavior during the CTOD test is shown in Fig. 4. Under the ambient air environment, the interface between the fatigue pre-crack and the propagating zone is visually divided into three distinct regions: the fatigue pre-crack region, stretch zone, and stable crack growth regions, as shown in Fig. 4(a). The microscopic fracture characteristics of the propagation region are illustrated by a completely ductile fracture morphology with dimples. The crack-blunting deformation behavior of the fatigue pre-crack tip can be observed from the side view of the haft specimen. This image was obtained at the middle location of the crack front after forced opening, polishing, and etching. A significant alteration of the crack tip fracture behavior under the 1 % H_2 gas

mixture is shown in Fig. 4(c). Mechanically, the CTOD can be evaluated directly using crack tip parameters such as the width and angle of the crack propagation direction of the stretch zone face. Some micro-voids are also observed ahead of the crack tip. The stretch zone was not visually observed, and the transition region between the fatigue pre-crack region and the propagating zone exhibits a pronounced crack. The dimples in the propagation zone have disappeared, and the fracture surface exhibits typical hydrogen-induced brittleness with a quasi-cleavage fracture mode. Based on the results obtained in this SEM fractography analysis, an illustration of the influence of hydrogen on the crack tip deformation and initiation is depicted schematically in Figs. 4(b) and (d). Extensive crack tip blunting can reduce the stress concentration at the crack tip; correspondingly, the CTOD is much larger when tested in ambient air. On the other hand, in the presence of hydrogen, the crack propagation is pronounced owing to hydrogen-promoted strain localization, resulting in the formation of hydrogen-assisted crack initiation on either side of the crack tip. The obtained results are also consistent with those reported in the literature, which indicate that a remarkable loss of fracture toughness often occurs in harsh environments containing hydrogen [31-33].

2.3 Effect of hydrogen on the fatigue crack growth properties

A comparison of the FCGR properties obtained in ambient air and under 1 % H_2 is presented in Fig. 5. In addition, the results are also compared to those obtained under 100 % H_2 at 10 MPa [34]. It can be seen that the relationship between the FCGR and the stress intensity factor range, ΔK, is expressed well as a straight line on a log-log plot with high confidence. The distinction between the results tested in ambient air and under 1 % H_2 is demonstrated by the presence of two separate regression lines. In particular, the FCGRs of the tests performed in the 1 % H_2 gas mixture condition were approximately an order of magnitude greater than those obtained under ambient air. In addition, the present results are also compared to that in 10 MPa of 100 % H_2, which was reported in previous research [34]. It is observed that the FCGR tested under 10 MPa of 100 % H_2 was little greater than that tested in 1 % H_2. These results are consistent with those in the literature, which also reported that hydrogen enhances the FCGR. The values of C and m, which are used to investigate the fatigue life, are listed in Table 3.

Fig. 6 presents a comparison of the fracture characteristics obtained for the fatigue crack growth tests in ambient air and under the 1 % H_2 gas mixture. Striations can be clearly distinguished on the fracture surface of the specimens tested in ambient air. However, in the tests performed in the 1 % H_2 gas mixture, it can be virtually impossible to distinguish the striation forms, and the fracture surface exhibits a complete quasi-cleavage fracture. In addition, the spacing of these striations is more pronounced at higher ΔK than at low ΔK when tested in

Table 3. Summary of the calculated Paris constants for X70 pipeline steel base and weld under different test conditions.

Material	Test condition	C	m
Base metal	atm, RT	2.06E-12	3.15
	1 % H_2 % & 1 % H_2 – 720h	1.26E-11	3.20
Weld metal	atm, RT	7.18E-13	3.46
	1 % H_2 % & 1 % H_2 – 720h	1.26E-12	3.82

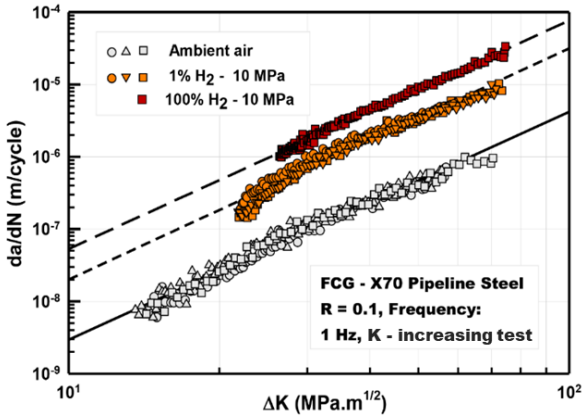

Fig. 5. Fatigue crack growth properties of API X70 pipeline steel under three environmental conditions.

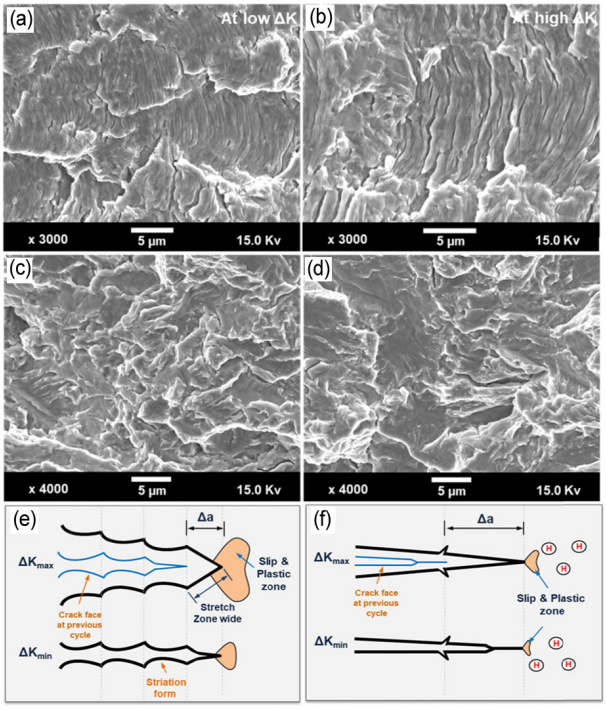

Fig. 6. Change in the fatigue fracture morphology under two hydrogen-containing environments: (a) at low ΔK under ambient air; (b) at high ΔK under ambient air; (c) under 1 % H_2 gas mixture at 10 MPa; (d) under 100 % H_2 at 10 MPa; schematic representations of the fatigue fracture morphologies under; (e) ambient air; (f) a hydrogen-containing environment.

ambient air. Schematic illustrations of the fatigue crack growth behavior under ambient air and in an environment containing hydrogen are depicted in Figs. 6(e) and (f). The fatigue crack growth mechanism is generally attributed to the formation of a plastic zone region ahead of the crack tip, resulting in either blunting or re-sharpening during cyclic loading. Under ambient air, an increment of fatigue crack propagation is a result of the formation of the stretch zone at the maximum loading stage. When the applied load changes to the minimum state, the slip direction and plastic deformation zone at the crack tip are reversed, resulting in crack tip re-sharpening. According to this mechanism, the amount of crack growth during one cycle can be evaluated through measurement of the corresponding striation spacing. On the other hand, the plastic zone and localized slip deformation remain relatively small owing to the hydrogen-enhanced decohesion embrittlement (HEDE) mechanism, resulting in a sharp crack and a larger crack growth increment per cycle [35-37]. It is suggested that the fracture mechanism in the maximum loading stage in one fatigue cycle during cyclic loading in either ambient air or an environment containing hydrogen can be considered comparable to the fracture mechanism during fracture toughness testing. However, the more severe loading conditions during the CTOD testing resulted in a more pronounced stretch zone and hydrogen-assisted cracking, which could be observed visually on the millimeter scale as shown in Fig. 4.

3. Fatigue life assessment

3.1 Assessment procedure

The internal surfaces of pressurized components are often considered the most critical locations in structural pipes because they are often exposed directly to harsh environments. A leak before break is more likely to occur in a situation with an internal surface flaw. Therefore, the remaining life assessment often focuses on a suggested model with an existing defect located at the interior surface. Based on the design fatigue life calculation, it is assumed that the crack propagation will start from the first pressure cycle. When the crack growth rate is in the mid-growth rate regime, the relationship between the amount of fatigue crack growth per cycle, *da/dN*, and the stress intensity factor range, *ΔK*, is generally described as a power function (Paris's law):

$$\frac{da}{dN} = C\left(\Delta K\right)^m \tag{2}$$

where *C* and *m* are constants, and *ΔK* can be written as

$$\Delta K = F\,\Delta\sigma\sqrt{\pi a} \tag{3}$$

where *Δσ* and F are the stress range and boundary correction factor of the crack model, respectively. The stress intensity factor range, *ΔK*, is defined as the difference between the maximum and minimum *K* at the crack tip, as shown in Eq. (3). Therefore, Eq. (2) can be written as:

$$\frac{da}{dN} = C\left(F\,\Delta\sigma\sqrt{\pi a}\right)^m \tag{4}$$

Then,

$$\int_{a_o}^{a_f}\frac{da}{a^{m/2}} = C\,F^m\left(\Delta\sigma\right)^m\pi^{m/2}\int_{o}^{N_f}dN \tag{5}$$

$$N_f = \frac{2}{\left(m-2\right)CY^m\left(\Delta\sigma\right)^m\pi^{m/2}}\left[\frac{1}{\left(a_o\right)^{(m-2)/2}} - \frac{1}{\left(a_f\right)^{(m-2)/2}}\right] \tag{6}$$

where *C* and *m* are the fatigue crack growth rate properties. These were obtained from the curves in Fig. 5 using the least squares method, and the corresponding results are presented in Table 2. The initial crack depth was determined based on the ability of the nondestructive method to detect small cracks or defects in the pressure vessel component. According to KHK 0220 [38], the suggested initial crack depth, a_o, is dependent on the wall thickness, *t*, as follows: a_o = 0.5 mm when $t \le 16$ mm, a_o = 1.1 mm when $16 \le t \le 51$ mm, and a_o = 1.6 when $t \ge 51$ mm. The initial crack aspect ratio, which is determined as the depth/length ratio, is assumed to be a/c = 1/3; this ratio is supposed to remain constant during crack propagation. It is noted that the crack aspect ratio may vary continuously during the crack propagation process. In future works, the effect of the aspect ratio values should be analyzed in order to ensure the reliability of the obtained results. On the other hand, the critical size is defined as either the cumulative crack size when $Ki \le K_{IC}$ (ASME Section VIII, Division - 10) [39] or the crack size equal to 80 % of the wall thickness (KHK 0220 - standard), whichever occurs first. Therefore, the unknown variables in Eq. (6) are mainly a function of the stress range and the boundary correction function of the crack model.

In general, the actual defects existing in structural pipelines are usually irregular in shape. These complex shapes may result in difficulties in evaluating the crack growth behaviors as well as the reliability of the life assessment. Based on historical service experience, most typical flaws in high-pressure vessels are assumed to have an elliptic surface shape located in the radial-axial plane (i.e., axial/circumferential internal semi-elliptical surface crack) (as shown in Fig. 7(b)) or appear as a radial-circumferential through-thickness flaw (i.e., radial/circumferential internal semi-elliptical surface crack), as shown in Fig. 7(c), on the internal surface of the vessel [40-42]. The crack parameters are defined based on the depth of the crack (*a*), half-length of the crack (c), pipe thickness (t), internal diameter of the pipe (R_i), and outer diameter of the pipe (R_o). In general, the deepest point is the most critical location along the crack front, at which the estimated fatigue life can be used to represent the most conservative life of the pipeline structure.

The stress intensity factor, *K*, for a surface flaw can be de-

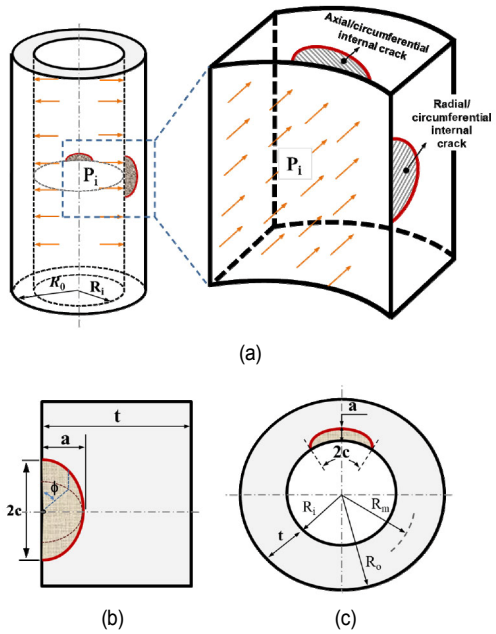

Fig. 7. (a) Geometric parameters of the proposed crack models; (b) detail of the crack geometry of an axial/circumferential internal semi-elliptical surface crack in a cylinder; (c) detail of the crack geometry of a radial/circumferential internal semi-elliptical surface crack in a cylinder.

termined from the internal pressure, *P*, and wall thickness using the analytical solution or simulations. The most well-known solution for the K of an elliptic surface crack located in the radial-axial plane on the internal surface of a thick-walled cylinder was derived by Newman and Raju [43, 44] as follows:

$$K=\sigma\sqrt{\pi\frac{a}{Q}}F\left(\frac{a}{t},\frac{a}{c},\frac{t}{R_i},\varphi\right) \tag{7a}$$

where σ is the remote tensile stress, *F* is the boundary correction factor, and *Q* is the shape factor for the elliptical crack. The ratio between the crack depth (a) and the half the crack length, (c) on the surface can be defined as the aspect ratio, (a/c) while the crack depth ratio (a/t) is defined as the ratio of the crack depth to the thickness of the pressure vessel. Because the surface crack located in the axial/radial plane on the internal surface grows mainly due to the hoop stress in a pressurized cylinder, the remote stress function can be written as follows:

$$\sigma_h=\frac{P_iR_i}{t} \tag{7b}$$

The shape factor for an elliptical crack, *Q*, can be approximated using Eq. (7c):

$$Q=1+1.464\left(\frac{a}{c}\right)^{1.65} \tag{7c}$$

The dimensionless *F* function for the external axial surface crack depends on the crack parameters. The integrated function for *F* is numerically defined as follows:

$$F=0.97\left[m_1+m_2\left(\frac{a}{t}\right)^2+m_3\left(\frac{a}{t}\right)^4\right]f_\varphi g\, f_c \tag{7d}$$

$$m_1=1.13-0.09\left(\frac{a}{c}\right) \tag{7e}$$

$$m_2=-0.54-\frac{0.89}{0.2+\frac{a}{c}} \tag{7f}$$

$$m_3=0.5-\frac{1.0}{0.65+\frac{a}{c}}+14\left(1-\frac{a}{c}\right)^{24} \tag{7g}$$

$$f_\varphi=\left[\left(\frac{a}{c}\cos\varphi\right)^2+\sin^2\varphi\right]^{\frac{1}{4}} \tag{7h}$$

$$g=1+\left[0.1+0.35\left(\frac{a}{t}\right)^2\right](1-\sin\varphi)^2 \tag{7i}$$

$$f_c=\left[\frac{\left(1+k^2\right)}{1-k^2}+1-0.5\sqrt{\nu}\right]\left(\frac{t}{R_i}\right) \tag{7j}$$

On the other hand, the radial–circumferential surface cracks propagate mainly because of axial stress in a pressurized cylinder. The solution for the stress-intensity factor *F* of a radial partial through-wall flaw was developed by Zahoor [45] as follows:

$$K=\sigma\sqrt{\pi a}\,F\left(\frac{a}{t},\frac{a}{c},\frac{t}{R_i},\varphi\right) \tag{8a}$$

where σ is defined as a function of the radial stress under the effect of internal pressure.

$$\sigma_t=\frac{P_iR_i}{2t} \tag{8b}$$

The boundary correction factor F is defined as:

$$F=1.1+\left[0.15241+16.772\left(\frac{a}{t}\frac{\theta}{\pi}\right)^{0.855}+14.944\left(\frac{a}{t}\frac{\theta}{\pi}\right)\right]\frac{a}{t} \tag{8c}$$

$$\theta=\frac{c}{R_i} \tag{8d}$$

The variables are defined in the same manner as for the case of the semi-elliptical crack in the axial direction.

Fig. 8 presents a schematic algorithm for the fatigue life assessment of an inner surface crack in a pipeline. At the beginning stage, a suitable range of geometric variables, operation

Table 4. Pressure range and parametric dimensions of the pipeline steel considered in the design fatigue life evaluation.

Design pressure, MPa	8, 10, 12, 15, 21
Pipe diameter, mm (inch)	610 (24), 660 (26), 762 (30), 1000 (40)
Pipe thickness, mm	11.9, 14.3, 15.9, 17.5

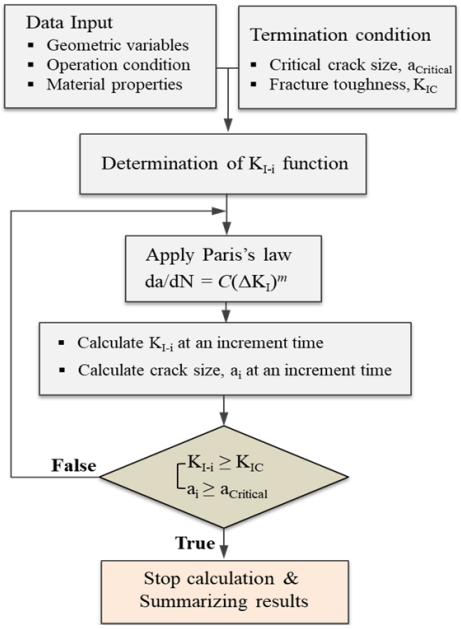

Fig. 8. Algorithm for the fatigue life assessment of an inner surface crack in a pipeline [40].

conditions, material properties, and terminal conditions must be determined. Based on the assumption of equivalent cracks in the components, the stress intensity factor function is determined based on the corresponding crack model. Then, based on the assumption of an appropriate time step, the increment of the crack length is calculated based on the stress intensity factor function and FCGR properties. Finally, the terminal condition of the slope is evaluated based on a comparison of the accumulated crack length and the critical crack length values.

This result mainly focuses on investigating the effect of a 10 MPa environment containing hydrogen on the design fatigue life of a natural gas pipeline with an outer diameter of 762 mm and wall thickness of 15.9 mm. For improved applicability, the fatigue life evaluation is also extended to the cover fluctuations in the pressure from 8 MPa up to the maximum allowable pressure of the pipeline of 21 MPa and variations in the design parameters of the pipeline, such as the pipe diameter and thickness. All of the analysis cases are summarized in Table 4. Based on the pre-calculation of K with Eqs. (7a) and (8a), using the terminal conditions in KHK0220 will provide a more conservative fatigue life prediction compared with the conditions in ASME because the value of the critical crack size when K_I at the deepest crack location equals K_{IC} is much larger than 80 % of the wall thickness of the pipe under all three environmental conditions. Therefore, the terminal condition for the

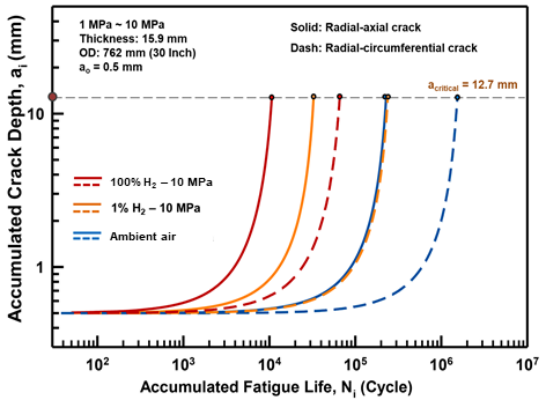

Fig. 9. Crack depth growth behavior as a function of fatigue life under various environmental conditions in two crack models for an initial crack depth of 0.5 mm and a crack aspect ratio, a/c, of 1/3.

crack size in the following calculations will adopt the KHK0220 regulation, which was described previously. It is noted that it is possible to trace the crack propagation process in both the depth and length directions.

3.2 Evaluation of fatigue life

Fig. 9 presents an illustration of the fatigue life calculation for a structural pipeline with an outer diameter of 762 mm and wall thickness of 15.9 mm under ambient air, 10 MPa of 1 % H_2, and 10 MPa of 100 % H_2 with both crack models and an initial crack depth of 0.5 mm. For each calculation, the estimated fatigue life is defined as when the accumulated crack size reaches 12.5 mm, which is equal to 80 % of the wall thickness. As can be seen, the fatigue life under 1 % H_2 at 10 MPa is approximate 3 times longer than that under 100 % H_2 at 10 MPa, while it is much shorter than that under ambient air conditions in both crack models. For example, under the radial-axial crack model, the design fatigue life under ambient air is more than 164000 cycles, while it is significantly decreased to less than 23000 cycles in 1 % H_2 at 10 MPa and less than 8000 cycles under 100 % H_2 at 10 MPa.

Fig. 10 presents the variations in the estimated design fatigue life with different initial crack sizes under three environmental conditions with two crack models when the pipe thickness is 15.9 mm and the outer diameter is 762 mm. When the initial crack size is small, the estimated fatigue life decreases gradually and almost linearly with increasing initial crack size under the three environmental conditions in both crack models, while the rate of decrease becomes much steeper in the second stage as the crack depth increases further. From these results, it can be argued that the crack propagation process during the small crack stage can dominate the total fatigue life. Comparing the two crack models, it can be seen that the fatigue life in the radial-axial crack model (represented by the solid line) is much longer than that in the radial-circumferential model (represented by the dashed line) under the three environmental conditions. Therefore, under actual conditions, pres-

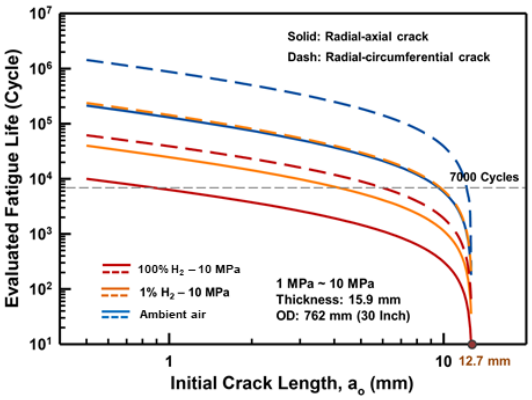

Fig. 10. Variation in the estimated design fatigue life with different initial crack sizes under three environmental conditions with two crack models for a fixed pipe thickness of 15.9 mm and outer diameter of 762 mm.

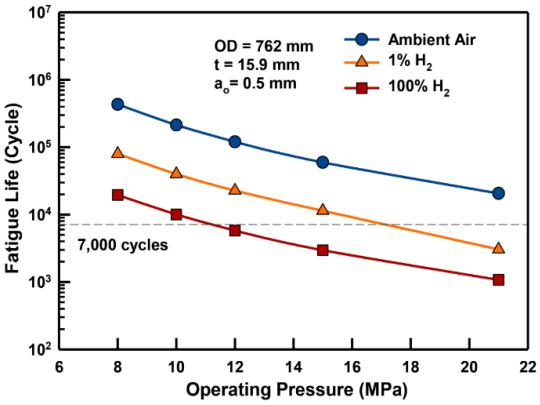

Fig. 11. Pressure dependency of the design fatigue life of X70 pipeline steel under three environmental conditions for a pipe thickness of 15.9 mm and initial crack size of 0.5 mm.

surized components with a radial-axial surface crack from the inner surface are in a more dangerous situation than those with a radial-circumferential surface crack model. Therefore, for more conservative remaining life assessment results, it is necessary to focus the analyses on the radial-axial crack model, which represents the worst-case scenario in actual operating conditions.

Fig. 11 shows the change in the estimated fatigue life of the radial-axial crack model with varying operating pressures from 8 MPa to 21 MPa under three environmental conditions for a pipe thickness of 15.9 mm and initial crack size of 0.5 mm. It can be seen that the fatigue life sharply decreases with increasing operating pressure in the range from 8 MPa to 21 MPa. In general, the fatigue life requirement of a structural component usually depends on the characteristics of the actual operating conditions. In general, ASME B31.3 [46] recommends that the design fatigue life requirement for a structural pipeline should be approximately 7000 cycles. As shown in Fig. 7, the estimated fatigue life under ambient air is greater than 7000 cycles for the entire pressure range. However, to satisfy the ASME requirement, the working pressure cannot exceed 16.5 MPa under a 1 % H_2 gas mixture, while it may not be practical to use X70 pipeline steel as a structural material when the pressure exceeds 11.75 MPa in a 100 % H_2 environment.

In general, a series of mechanical tests, such as slow strain rate tensile and fatigue life tests, are typically required to establish quantitatively that a material is eligible for hydrogen service. Depending on the typical working conditions of these structures, additional tests are often required, and a quantitative evaluation of the synergistic action in the experimental results is often considered. Based on the above results, it is found that the design fatigue life of practical materials is not only sensitive to environmental conditions, but also changes according to variations in the operating pressure and the geometric parameters. ASME Section VIII, Division 3 regulates the design pressure, pipe thickness, and diameter of a pressurized component according to the properties of the material used [39]. In the comparison of the influence of those factors, it can be seen that the effect of the operating pressure on the design fatigue life is more pronounced than the effects of varying the outer diameter or pipe thickness, as shown in Figs. 11-13. As mentioned above, the evaluated fatigue life of X70 pipeline steel under the practical parameters of a pipeline system is asymptotic to the standard design requirement even under a pure hydrogen environment. At present, pipelines are considered as the lowest-cost transportation system for water electrolytic hydrogen, which can replace NG in existing pipeline systems [47]. However, the widespread commercialization of API pipeline steel for storing and transporting H_2 is still highly hazardous under current regulations and standards, as this group of high-strength low-alloy steels are categorized as extremely embrittled materials owing to their high degree of susceptibility [48, 49]. Thus, this application may be accompanied by extensive upgrades and high costs.

It is noted that the estimated fatigue life results depend not only on the operating pressure of the pipe, but also on the mechanical performance, such as the fracture toughness and fatigue crack growth rate properties of materials tested under the same operating pressure. Experimental FCGR data obtained at pressures higher than 10 MPa H_2 are not available. Therefore, all of the fatigue life evaluations at hydrogen pressures of greater than 10 MPa have been carried out based on the assumption that the fracture toughness and FCGR properties tested at higher pressures will be similar to those tested under 10 MPa in a hydrogen-containing environment. Even though the environmental hydrogen-assisted FCGR may reach a plateau when the pressure is higher than 5.5 MPa, the fatigue crack growth properties under higher pressures may also be accelerated, especially under a 1 % H_2 gas mixture, owing to the increase in the partial hydrogen pressure [48]. Therefore, the fatigue life in the actual hydrogen condition above 10 MPa H_2 may be shorter than the estimated values in the present study. Additionally, it should be noted that the FCGRs are also dependent on the loading ratio, and the general trend is that the FCGR is accelerated at higher loading ratios [9, 15, 50]. The fluctuation in the operating pressure is also not constant at 0.1. These effects were not directly accounted for in this re-

search. Therefore, additional FCGRs at higher pressures and under varying loading ratios are required to provide more efficient and accurate data for the evaluation of the failure pressure of steel pipelines.

Moreover, a large number of cycles can occur during the development process from a blunt notch to crack initiation in actual operating conditions, whereas the fatigue life assessment often assumes that the initial flaw has a very sharp notch and crack propagation will occur in the first cycle. In this circumstance, the estimated fatigue life seems to be too conservative. Furthermore, a large portion of the fatigue crack propagation life is in the small-crack stage, and thus it is critically important to choose an appropriate initial crack size, as the assumption of the initial small crack will significantly affect the prediction of the total fatigue life. Therefore, in the life assessment of in-service pressurized structures, controlling the initial crack depth is an effective means to enhance the design fatigue life of pressurized components. The estimated fatigue life results are adequate to withstand the fluctuation in operating pressure and varying pipe geometries in the practical range. Extensive consideration of the effect of the loading ratio, the effect of a blunting notch before crack propagation, and the pressure dependency of the FCGR should be further analyzed to provide more accurate results.

4. Conclusions

The influence of a low partial hydrogen in a hydrogen/natural gas mixture on the crack tip deformation behavior and the fracture toughness of X70 pipeline steel was investigated. Based on the results obtained for the fracture parameters, an analytical procedure for the fatigue life assessment was established. The following conclusions can be drawn:

Both base and weld metal exhibits a significant degradation in fracture resistance as expressed in CTOD reduction when tested under 1 % H_2 gas mixture conditions. The reduction trend in the base metal is consistent with that in the weld metal. The CTOD remarkably dropped by more than 55 % compared to that in the ambient air. The fracture toughness of the specimen tested in a 10 MPa gas mixture with 1 % H_2 was decreased by 30 % compared to the specimen tested in ambient air.

The FCGR was markedly accelerated under the 1 % hydrogen blend gas mixture compared with the tests performed in ambient air. The trend of enhancement in FCGR in 1 % hydrogen was observed to be of the same order in both base metal and weld specimens within the experimental ΔK range in this study. The accompanying change in the fracture mechanism under the 1 % H_2 gas mixture conditions was discussed.

The estimated fatigue life of the structural pipeline under 1 % H_2 gas mixture conditions is much shorter than that under ambient air owing to the decrease in fracture toughness and acceleration of the FCGR. A large portion of the fatigue crack propagation life takes place in the small-crack stage; therefore, the estimated fatigue life is strongly affected by the initial crack initiation size. The radial-axial surface crack model from the inner surface was more dangerous than the radial-circumferential crack model.

Acknowledgments

This research was supported by Development of Reliability Measurement Technology for Hydrogen Refueling Station funded by Korea Research Institute of Standards and Science (KRISS-2020-GP2020-0007).

Nomenclature

a : Crack depth
a_o : Initial crack depth
$a_{Critical}$: Critical crack depth
C : Fatigue crack growth coefficient
c : Half of crack length
$CTOD$: Crack tip opening displacement
F : Boundary correction
$FCGR$: Fatigue crack growth rate
K : Stress intensity factor for mode I crack
K_{IC} : Fracture toughness
m : Fatigue crack growth exponent
P : Internal pressure
Q : Shape factor
R_i : Inner radius of cylinder
R_m : Mean radius of cylinder
R_o : Outer radius of cylinder
t : Wall thickness of cylinder
σ : Stress and stress rate, respectively
σ_h : Hoop stress in cylinder
σ_r : Axial stress in cylinder

References

[1] E. J. Moniz, H. D. Jacoby, A. J. Meggs, R. C. Armtrong, D. R. Cohn, S. R. Connors and G. M. Kaufman, *The Future of Natural Gas*, Cambridge, MA: Massachusetts Institute of Technology (2011).

[2] J. G. Speight, *Natural Gas: A Basic Handbook*, Gulf Professional Publishing (2018).

[3] D. Hardie, E. A. Charles and A. H. Lopez, Hydrogen embrittlement of high strength pipeline steels, *Corros. Sci*., 48 (2006) 4378-4385.

[4] Y. Zhao and M. Song, Failure analysis of a natural gas pipeline, *Eng. Fail. Anal*., 63 (2016) 61-71.

[5] E. S. Meresht, T. S. Farahani and J. Neshati, Failure analysis of stress corrosion cracking occurred in a gas transmission steel pipeline, *Eng. Fail. Anal*., 18 (2011) 963-970.

[6] H. B. Xue and Y. F. Cheng, Characterization of inclusions of X80 pipeline steel and its correlation with hydrogen-induced cracking, *Corros. Sci*., 53 (2011) 1201-1208.

[7] G. Ghosh, P. Rostron, R. Garg and A. Panday, Hydrogen induced cracking of pipeline and pressure vessel steels: a review,

Eng. Fract. Mech., 199 (2018) 609-618.
[8] A. Mustapha, E. A. Charles and D. Hardie, Evaluation of environment-assisted cracking susceptibility of a grade X100 pipeline steel, *Corros. Sci*., 54 (2012) 5-9.
[9] B. P. Somerday, P. Sofronis, K. A. Nibur, C. San Marchi and R. Kirchheim, Elucidating the variables affecting accelerated fatigue crack growth of steels in hydrogen gas with low oxygen concentrations, *Acta Mater*., 61 (2013) 6153-6170.
[10] H. J. Cialone and J. H. Holbrook, Effects of gaseous hydrogen on fatigue crack growth in pipeline steel, *Metall. Trans. A*, 16 (1985) 115-122.
[11] I. Moro, L. Briottet, P. Lemoine, E. Andrieu, C. Blanc and G. Odemer, Hydrogen embrittlement susceptibility of a high strength steel X80, *Mater. Sci. Eng. A*, 527 (2010) 7252-7260.
[12] L. Gan, F. Huang, X. Zhao, J. Liu and Y. F. Cheng, Hydrogen trapping and hydrogen induced cracking of welded X100 pipeline steel in H_2S environments, *Int. J. Hydrogen Energy*, 43 (2018) 2293-2306.
[13] R. L. Eadie, K. E. Szklarz and R. L. Sutherby, Corrosion fatigue and near-neutral pH stress corrosion cracking of pipeline steel and the effect of hydrogen sulfide, *Corrosion*, 61 (2005) 167-173.
[14] M. C. Zhao, M. Liu, A. Atrens, Y. Y. Shan and K. Yang, Effect of applied stress and microstructure on sulfide stress cracking resistance of pipeline steels subject to hydrogen sulfide, *Mater. Sci. Eng. A*, 478 (2008) 43-47.
[15] C. San Marchi, B. P. Somerday, K. A. Nibur, D. G. Stalheim, T. Boggess and S. Jansto, Fracture and fatigue of commercial grade API pipeline steels in gaseous hydrogen, *Proceedings from ASME 2010 Pressure Vessels and Piping Division*, Bellevue, Washington, USA (2010).
[16] L. Briottet, R. Batisse, G. de Dinechin, P. Langloi and L. Thiers, Recommendations on X80 steel for the design of hydrogen gas transmission pipelines, *Int. J. Hydrogen Energy*, 37 (2012) 9423-9430.
[17] C. Azevedo, Failure analysis of a crude oil pipeline, *Eng. Fail. Anal*., 14 (2007) 978-994.
[18] S. P. Lynch, Failures of structures and components by environmentally assisted cracking, *Eng. Fail. Anal*., 1 (1994) 77-90.
[19] M. Dadfarnia, P. Sofronis, J. Brouwer and S. Sosa, Assessment of resistance to fatigue crack growth of natural gas line pipe steels carrying gas mixed with hydrogen, *Int. J. Hydrogen Energy*, 44 (2019) 10808-10822.
[20] J. Capelle, J. Gilgert, I. Dmytrakh and G. Pluvinage, The effect of hydrogen concentration on fracture of pipeline steels in presence of a notch, *Eng. Fract. Mech*., 78 (2011) 364-373.
[21] R. Rebak, Z. B. Xia, R. Safruddin and Z. Szklarska-Smialowska, Effect of solution composition and electrochemical potential on stress corrosion cracking of X-52 pipeline steel, *Corrosion*, 52 (1996) 396-405.
[22] A. Díaz, J. M. Alegr and I. I. Cuesta, Numerical simulation of hydrogen embrittlement and local triaxiality effects in notched specimens, *Theoretical and Applied Fracture Mechanics*, 90 (2017) 294-302.
[23] M. Wang, E. Akiyam and K. Tsuzaki, Effect of hydrogen and stress concentration on the notch tensile strength of AISI 4135 steel, *Mater. Sci. Eng. A*, 398 (2005) 37-46.
[24] K. Ma, Z. Hua, C. Gu, Z. Zhang, S. Ye and Y. Yao, Effects of crack position on fatigue life of large seamless storage vessels made of 4130X for hydrogen refueling station, *Int. J. Hydrogen Energy*, 44 (2019) 22559-22568.
[25] Z. Li, X. Jiang, H. Hopman, L. Zhu and Z. Liu, An investigation on the circumferential surface crack growth in steel pipes subjected to fatigue bending, *Theoretical and Applied Fracture Mechanics*, 105 (2020) 102403.
[26] Z. Li, X. Jiang, H. Hopman, L. Zhu and Z. Liu, External surface cracked offshore steel pipes reinforced with composite repair system subjected to cyclic bending: an experimental investigation, *Theoretical and Applied Fracture Mechanics*, 109 (2020) 102703.
[27] *ISO 12135: 2002, Metallic Materials-unified Method of Test for the Determination of Quasistatic Fracture Toughness*, International Organization for Standardization (ISO) (2002).
[28] *ASTM E647-15, Standard Test Method for Measurement of Fatigue Crack Growth Rates,* ASTM International (2015).
[29] T. T. Nguyen, J. Park, W. S. Kim, S. H. Nahm and U. B. Beak, Effect of low partial hydrogen in a mixture with methane on the mechanical properties of X70 pipeline steel, *Int. J. Hydrogen Energy*, 45 (2020) 2368-2381.
[30] U. B. Beak, T. T. Nguyen, J. Park, W. S. Kim and S. H. Nahm, Hydrogen-induced fracture of X70 pipeline steel base/weld under natural/hydrogen gas mixture condition, *ASME 2020 Pressure Vessels and Piping Conference,* American Society of Mechanical Engineers, PVP2011-21361.
[31] G. Álvarez, A. Zafra, F. J. Belzunce and C. Rodríguez, Hydrogen embrittlement analysis in a CrMoV steel by means of sent specimens, *Theoretical and Applied Fracture Mechanics*, 106 (2020) 102450.
[32] L. B. Peral, A. Zafra, J. Belzunce and C. Rodríguez, Effects of hydrogen on the fracture toughness of CrMo and CrMoV steels quenched and tempered at different temperatures, *Int. J. Hydrogen Energy*, 44 (2019) 3953-3965.
[33] Y. Ogawa, H. Matsunaga, J. Yamabe, M. Yoshikawa and S. Matsuoka, Unified evaluation of hydrogen-induced crack growth in fatigue tests and fracture toughness tests of a carbon steel, *Int. J. Fatigue*, 103 (2017) 223-233.
[34] U. B. Baek, H. M. Lee, S. W. Baek and S. H. Nahm, Hydrogen embrittlement for X-70 pipeline steel in high pressure hydrogen gas, *ASME 2015 Pressure Vessels and Piping Conference,* American Society of Mechanical Engineers, PVP2015-45475.
[35] S. Lynch, Discussion of some recent literature on hydrogen-embrittlement mechanisms: addressing common misunderstandings, *Corrosion Reviews*, 37 (2019) 377-395.
[36] D. Birenis, Y. Ogawa, H. Matsunaga, O. Takakuwa, J. Yamabe, Ø. Prytz and A. Thøgersen, Interpretation of hydrogen-assisted fatigue crack propagation in BCC iron based on dislocation structure evolution around the crack wake, *Acta Mater*., 156 (2018) 245-253.
[37] A. Nagao, C. D. Smith, M. Dadfarnia, P. Sofronis and I. M. Robertson, The role of hydrogen in hydrogen embrittlement fracture of lath martensitic steel, *Acta Mater*., 60 (2012) 5182-5189.

[38] KHKS 0220:2008. *Standard for Superhigh-pressure Gas Equipment*, Tokyo, Japan (2008).
[39] ASME Section VIII, Division 3 Code, 2007 Edition, Article Corsica, France. KD-10, *Special Requirements for Vessels in High Pressure Gaseous Hydrogen Transport and Storage service*, ASME, New York, NY.
[40] K. B. Yoon, T. G. Park and A. Saxena, Creep crack growth analysis of elliptic surface cracks in pressure vessels, *Int. J. of Pressure Vessels and Piping,* 80 (2003) 465-479.
[41] N. N. Tun, H. S. Yang, J. M. Yu and K. B. Yoon, Creep crack growth analysis using C t-parameter for internal circumferential and external axial surface cracks in a pressurized cylinder, *Journal of Mechanical Science and Technology,* 30 (2016) 5447-5458.
[42] B. Zakavi, A. Kotousov, A. Khanna and R. Branco, A new method for analysis of part-elliptical surface cracks in structures subjected to fatigue loading, *Theoretical and Applied Fracture Mechanics*, 103 (2019) 102258.
[43] S. Raju and J. C. Newman, Stress intensity factors for internal and external surface cracks in cylindrical vessels, *Journal of Pressure Vessel Technology*, 104 (1982) 293-298.
[44] J. Newman Jr. and I. Raju, An empirical stress-intensity factor equation for the surface crack, *Eng. Fract. Mech*., 15 (1981) 185-192.
[45] A. Zahoor, *Research Project 1757-69*, *Ductile Fracture Handbook*, Electric Power Research Institute (1990).
[46] *ASME B 31.8, Gas Transmission and Distribution Piping System*, New York: American Society of Mechanical Engineers (2004).
[47] C. Yang and J. Ogden, Determining the lowest-cost hydrogen delivery mode, *Int. J. Hydrogen Energy*, 32 (2007) 268-286.
[48] T. T. Nguyen, J. S. Park, W. S. Kim, S. H. Nahm and U. B. Beak, Environment hydrogen embrittlement of pipeline steel X70 under various gas mixture conditions with in situ small punch tests, *Mater. Sci. Eng. A* (2020) 139114.
[49] H. Matsunaga, M. Yoshikaw, R. Kondo, J. Yamabe and S. Matsuoka, Slow strain rate tensile and fatigue properties of Cr–Mo and carbon steels in a 115 MPa hydrogen gas atmosphere, *Int. J. Hydrogen Energy*, 40 (2015) 5739-5748.
[50] J. Ronevich, C. San Marchi, R. Kolasinski, K. Thurmer, N. Bartelt, F. El Gabaly and B. Somerday, Oxygen impurity effects on hydrogen assisted fatigue and fracture of X100 pipeline steel, *Pressure Vessels and Piping Conference*, American Society of Mechanical Engineers, 51685 (2018) V06BT06A027.

Thanh Tuan Nguyen received his Ph.D. in Mechanical Engineering from Chung-Ang University, Korea in 2018. He is currently working as a post-doctoral fellow at the Korea Research Institute of Standard and Science. His research interests are failure analysis, high-temperature fracture mechanics and the effect of gaseous hydrogen environments on the mechanical properties of materials.

Hyeong Min Heo received his Ph.D. in Material Science Engineering from Han Yang University, Korea in 2019. He is currently working as Senior Researcher at the Korea Research Institute of Standard and Science. His research interests are material characterizations and the mechanical behaviour of materials under the effect of hydrogen gas.

Jaeyeong Park received his Ph.D. in Material Science Engineering from Pohang University of Science and Technology, Korea in 2018. He is currently working as Senior Researcher at the Korea Research Institute of Standard and Science. His research interests are materials science and the mechanical behaviour of materials at high temperature, including anisotropic materials such as gas turbine blades.

Seung Hoon Nahm received his Ph.D. in Mechanical Engineering from Kyungpook National University, Korea in 1997. He is currently working as Principal Research Scientist at the Korea Research Institute of Standard and Science. His research interests are the mechanical behaviour of materials at the micro and nano-scales, hydrogen embrittlement and mechanical behaviour of materials at high temperature.

Un Bong Baek received his Ph.D. in Mechanical Engineering from Kyungpook National University in 2001. He worked at Georgia Institute of Technology, U.S.A. as a post-doctoral fellow during 2002-2003. Dr. Baek is currently Director of the Centre for Energy and Material Metrology of KRISS (Korea Research Institute of Standards and Science). His research interest is in the mechanical behaviour of materials in high-pressure hydrogen environments.